Earthquake Source Zones in Intraplate Australia without Binning

Malcolm Sambridge[1], Cvetan Sinadinovski[2] and Kevin McCue[3]

[1] BSc (Hons), PhD, Professor and Head of Seismology and Mathematical Geophysics, ANU, Canberra, Australia. Malcolm.Sambridge@anu.edu.au
[2] PhD, Dr Cvetan Sinadinovski, Seismologist, Saudi Aramco, KSA. cvetansin@hotmail.com
[3] BSc (Hons), DIC, MPhil, FIEAust, Adjunct Professor CQU. Australian Seismological Centre, Canberra, ACT, Australia, mccue.kevin@gmail.com

Abstract

Establishing boundaries around source zones, areas where earthquakes are thought to be related through geological structure, mechanism, common stress direction, activity rate or any other process, involves subjective decision making. To minimise subjectivity in the process we propose use of the Voronoi diagram of earthquakes as a basis of zoning and subsequent hazard assessment. The approach is novel in that it creates a partition of the surface, with one earthquake in each cell, and cell size inversely proportional to the density of seismicity. A feature of the Voronoi diagram is that a spatially variable density is quantified without imposing any spatial binning. In this sense calculations of Voronoi diagrams involve no subjective assumptions of any kind, but merely reflect the geographical distribution of seismicity. Decisions are still required on which seismic events the Voronoi diagram is built from, which may be a complete catalogue or after editing to eliminate foreshocks and aftershocks or other issues due to incompleteness.

We have utilised the 12,226 events in the Gibson earthquake database adopted by Geoscience Australia without attempting to convert magnitudes to Mw using any of the myriad conversion equations available, thus avoiding another subjective decision.

Binless earthquake log-density maps, have been created with different smoothing techniques with Voronoi polygon cells or Delaunay triangles to identify sets of like earthquakes. Our preferred smoother is to use linear interpolation applied to nine passes of a multi-scale averaging of nearest neighbor log-densities. This looks to be a reasonable starting point for defining source zones within a PSHA model of continental Australia.

Keywords: Nearest Neighbour algorithm, Voronoi cells, Australian earthquakes, PSHA

INTRODUCTION

Previous studies of earthquake zoning in Australia have used bins at different scales, polygon-shaped bins with or without smoothing or fuzzy boundaries (McCue; 1973, 1975; Gaull et al, 1990; Greenhalgh and McDougall, 1990); McCue 1993; McCue and others, 1993; Love, 1996; Cuthbertson and others, 1997; Leonard and others, 2012; Schäfer and Daniell, 2014; Schäfer and others, 2015), bins of variable volume such as geological structures of uniform age and composition (Brown and Gibson, 2004), bins of identified active faults (Clark and McPherson, 2012). The reader is referred to this papers for details of particular binning approaches.

A drawback of binning is that often the size and shape of the bins is a subjective choice. Too large or too small bins may under or over represent the spatial variability of the underlying quantity of interest. If identifying source zones is the goal then defining bins at the outset may strongly influence the shape of the output source zones. In this paper we investigate several methods to recover the density distribution of an irregularly spaced set of earthquake epicentres without imposing spatial binning. This is done using geometric concepts known as the Voronoi diagram (Voronoi, 1908; Okabe et al. 1992). In this way we are able to derive an estimate of earthquake density which is spatially varying and requires no subjective choice of length scale.

1 Earthquakes, Voronoi cells and densities

The distribution of epicentres of earthquakes across the Australian continent is highly irregular with separations varying over several orders of magnitude. Figure 1 shows the 12,226 events in Gibson's Australian earthquake database (pers. comm.) with magnitude greater than 2.5, from 1837 to 2014. Our interest is to derive quantities that depend on earthquake densities. A common way to plot an earthquake density map is to divide the region into uniform bins and count the number of earthquakes in each.

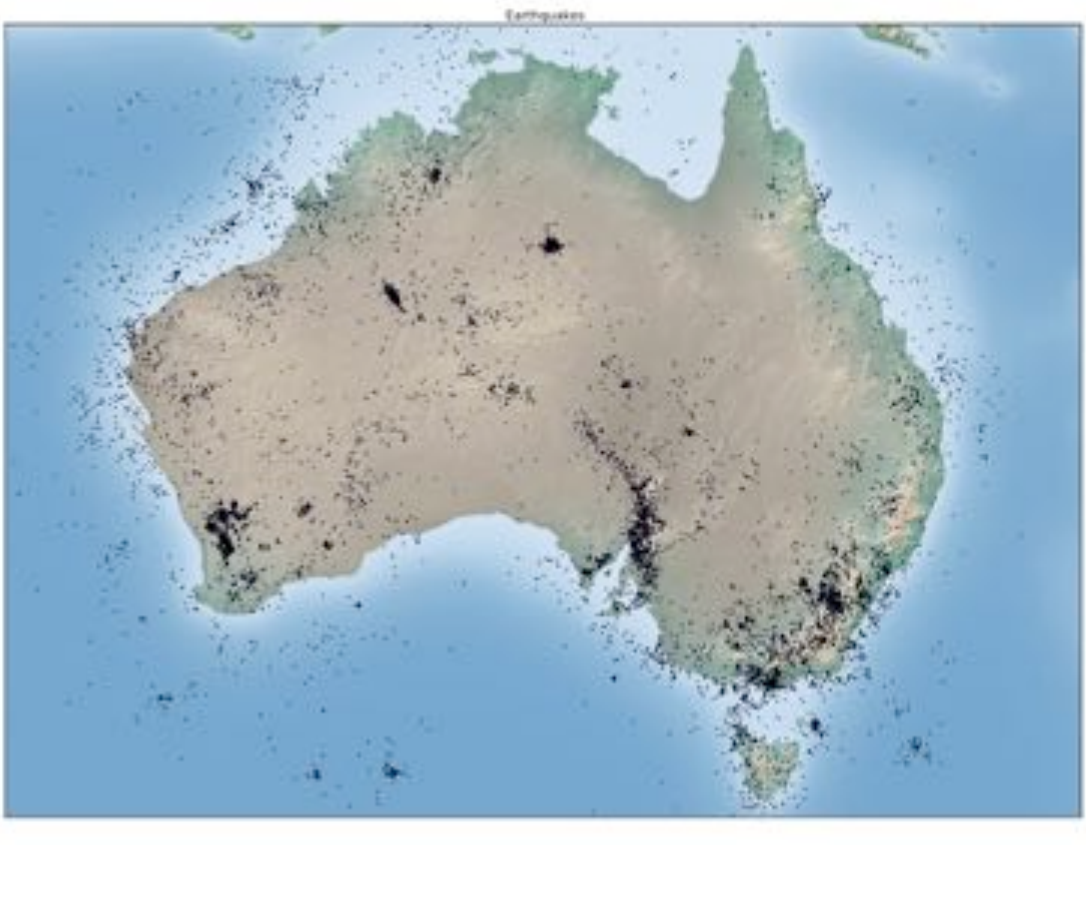

Figure 1 Earthquake epicentres from the Australian catalogue (Gibson pers. comm.) used in these experiments, some12,226 earthquakes.

This, while simple, has the disadvantage that the result can be heavily dependent on the size of the spatial bin. Too large a bin will smooth over observable variations in seismicity, while too small a bin may have too few earthquakes to get a reliable density estimate. Our paper explores a few alternate ways to recover an earthquake density map that do not require an arbitrary choice of spatial bin. We focus here only on epicentral densities, but in principle the same tools might be used to recover variations in other quantities, such as 'b-values' or probabilistic hazard measures.

Rather than count the number of earthquakes within a given spatial region, we make use of the properties of the Voronoi diagram (also know as Thiessen cells; Voronoi, 1908; Sambridge, 1995; https://en.wikipedia.org/wiki/Voronoi_diagram) that are nearest neighbour regions in the plane. Figure 2 shows an example of a Voronoi diagram built from 20 points, or nuclei, shown as dots in the plane. Each Voronoi cell covers the part of the plane that is closer to its defining nucleus than any other nucleus. A Voronoi cell is a polygon made up of edges, each of which is a perpendicular bi-sector of two corresponding nuclei. For a full treatment of Voronoi cells and their properties see Okabe and others, 1992. The size and shape of each Voronoi cell is only a function of the positions of the nuclei. Small results naturally result when points are close and large when they are far apart. The Voronoi diagram therefore forms a self-adaptive space filling tessellation of the plane that reflects the distribution of nuclei. Here we use the reciprocal of the area of each cell as a local measure of earthquake density. Note that Voronoi cells on the convex hull of the points, i.e. the outer perimeter have infinite Voronoi cells and hence zero density.

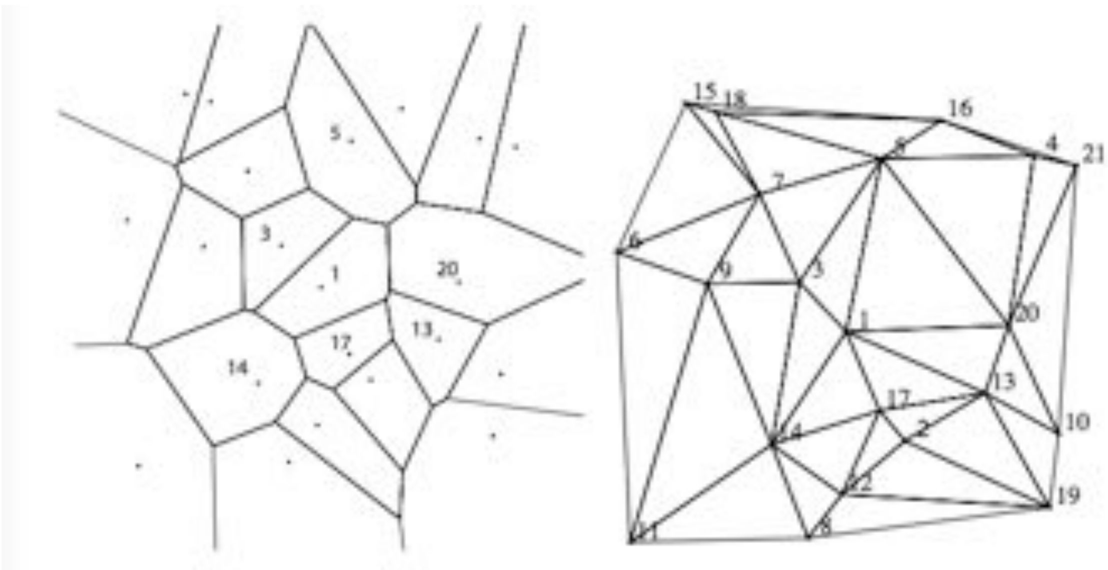

Figure 2 Voronoi diagram (left) showing nearest neighbour regions about a set of irregular points in the plane. Delaunay triangulation (right) joining nearest neighbour nuclei in the Voronoi diagram. The six numbered cells in the Voronoi diagram share a boarder with cell 1 and are its neighbours.

Figure 3 shows the Voronoi diagram of the 12,226 earthquakes in the Australian catalogue, a seismicity map of sorts. The size of the cells reflect the density of epicentres. Figures such as Figure 3 can be difficult to view because cell sizes vary over several orders of magnitude. Figure 4 shows the distribution of densities and log-densities respectively calculated in this way and why it is preferable to work with log-densities.

In what follows we describe several experiments to create an image of earthquake density. Except for the events on the convex hull (open cells at the edge) a density proxy is available for each earthquake epicentre. Here we focus only on testing different scattered data interpolation methods to recover an image across the region.

2 Interpolating densities

The rest of these notes describe a series of images produced with different scattered interpolation methods. We briefly describe and discuss each in turn. All images were produced using one of two python files. Using the interpolation methods we evaluated the image on either a 500x500 or 1000x1000 grid across the region.

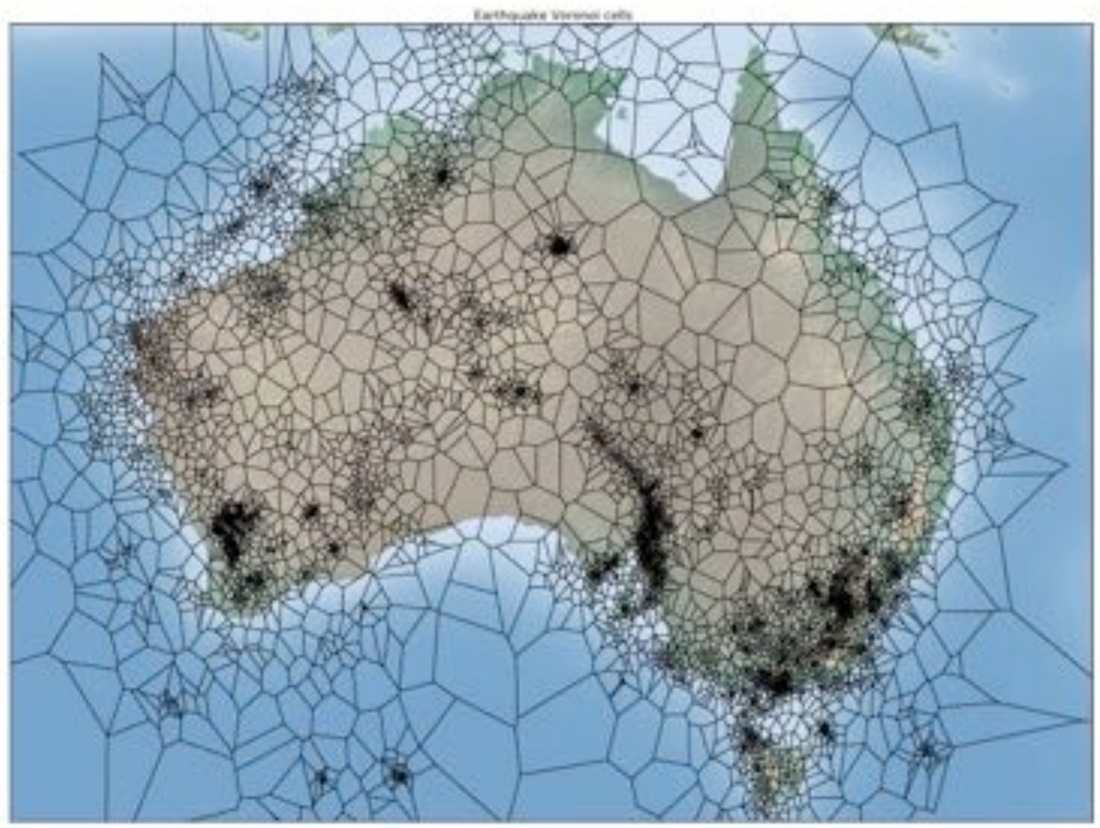

Figure 3 Voronoi diagram of 12,226 earthquake epicentres from the Australian catalogue (Gibson) shown in Figure 1. Cells with infinite area on the conex hull have been removed.

2.1 Constant density inside Voronoi cells

The first interpolation is simply to set the density a constant within each Voronoi cell. Figure 5 shows a plot of log-density produced in this way. In all plots the colour scale is the same which is linear in the log of the density rather than the density itself. This is because, as seen in Figure 4, the density varies by too many orders of magnitude to use a linear scale. In the same way that we interpolate the log-density proxy one could equally well apply the same procedure to any other scalar property associated with epicentral position. This image (Figure 5) consists of a series of polygonal regions which show trends in seismicity density but retains the multi-scale character of the density estimate.

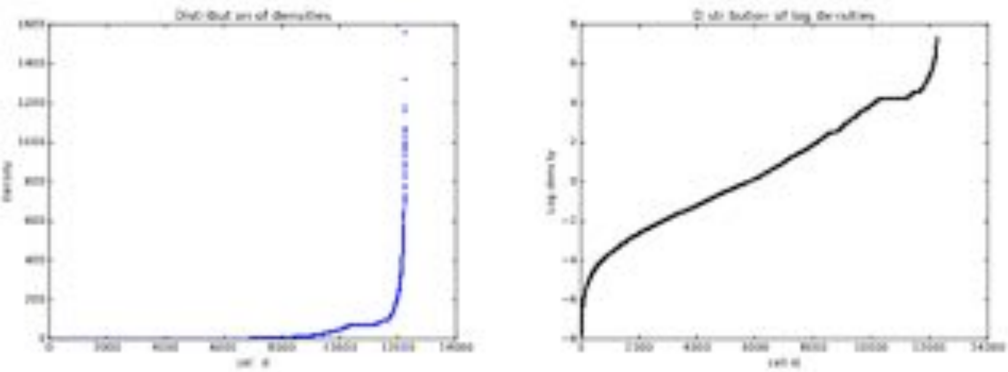

Figure 4 An ordered distribution of earthquake density (left) and log-density for the earthquake dataset, where density is set equal to the inverse of the Voronoi cell area about each earthquake in Figure 3.

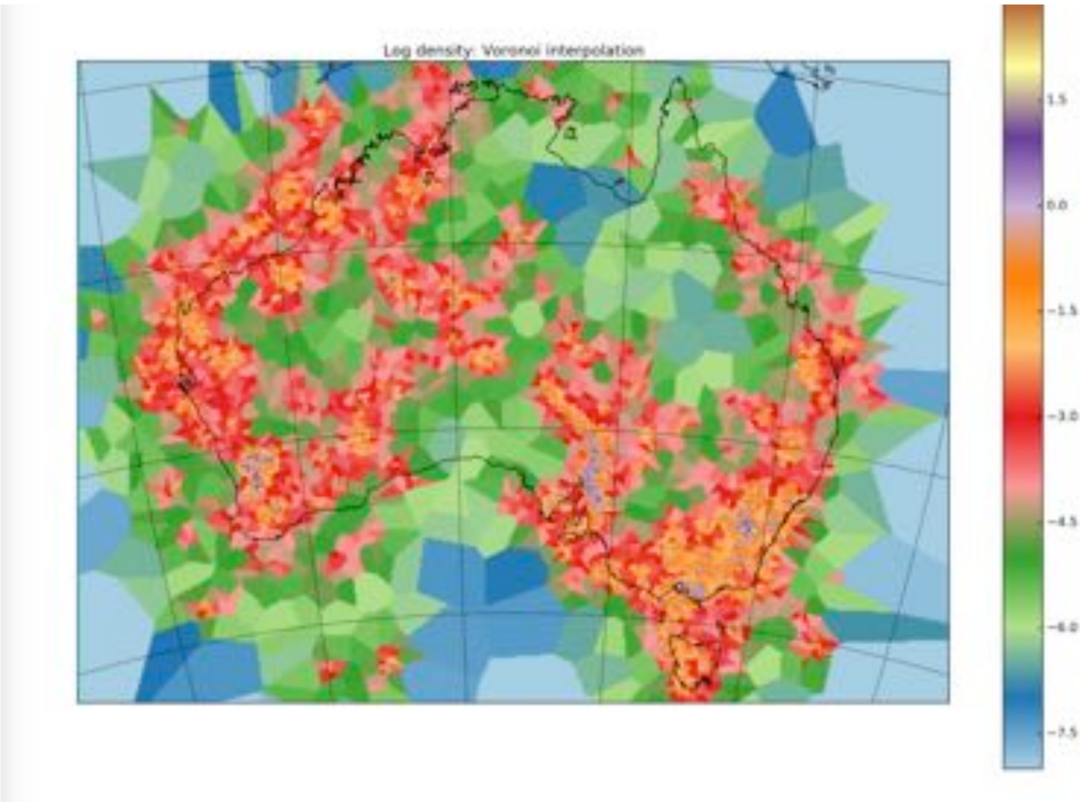

Figure 5 An interpolation of log-density proxy using a simple constant inside each Voronoi cell.

2.2 Linear interpolation in Delaunay triangles

The second interpolation is spatially linear inside a Delaunay triangulation of the earthquake epicentres. The Delaunay is a (nearly always unique) triangulation which is formed as the ‘dual’ of the Voronoi diagram, see Figure 5. For more information of Delaunay triangles see Sambridge (1995) and references therein.

Linear interpolation is straightforward inside each triangle using the log-density values known at each vertex, the earthquake epicentres. Figure 6 shows the corresponding image. This provides some gradient information on density variations which is missing in Figure 5 and as with all images retains a multi-scale character.

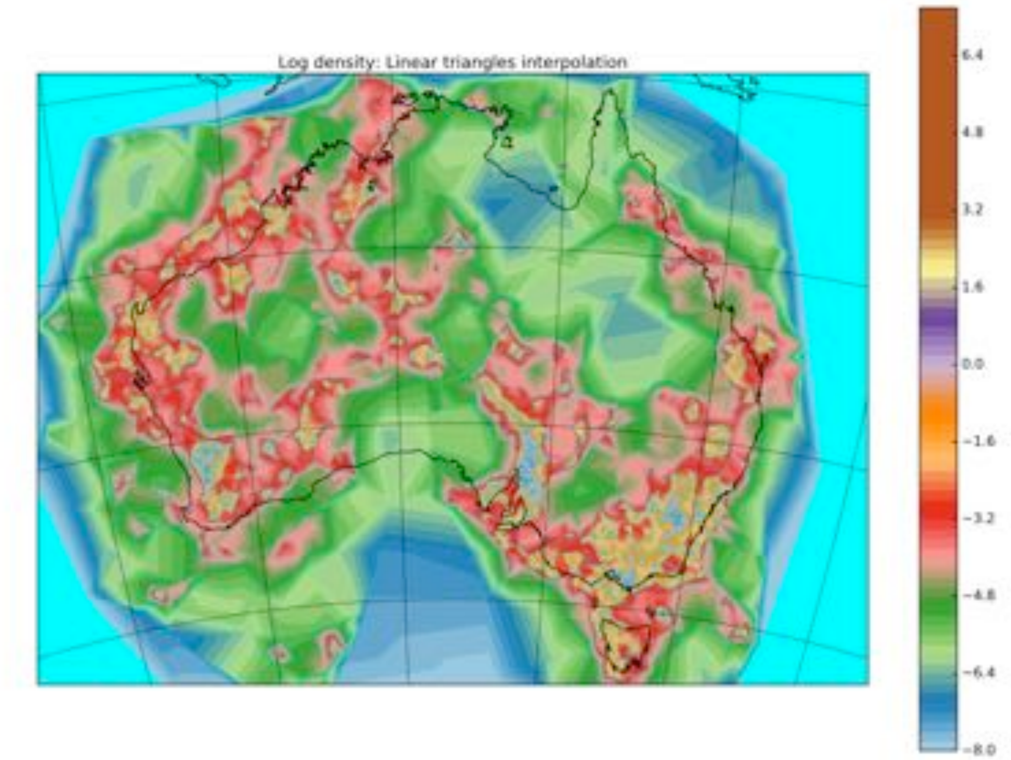

Figure 6 An interpolation of log-density proxy using a spatially linear interpolation inside each Delaunay triangle.

2.3 Bi-Linear interpolation

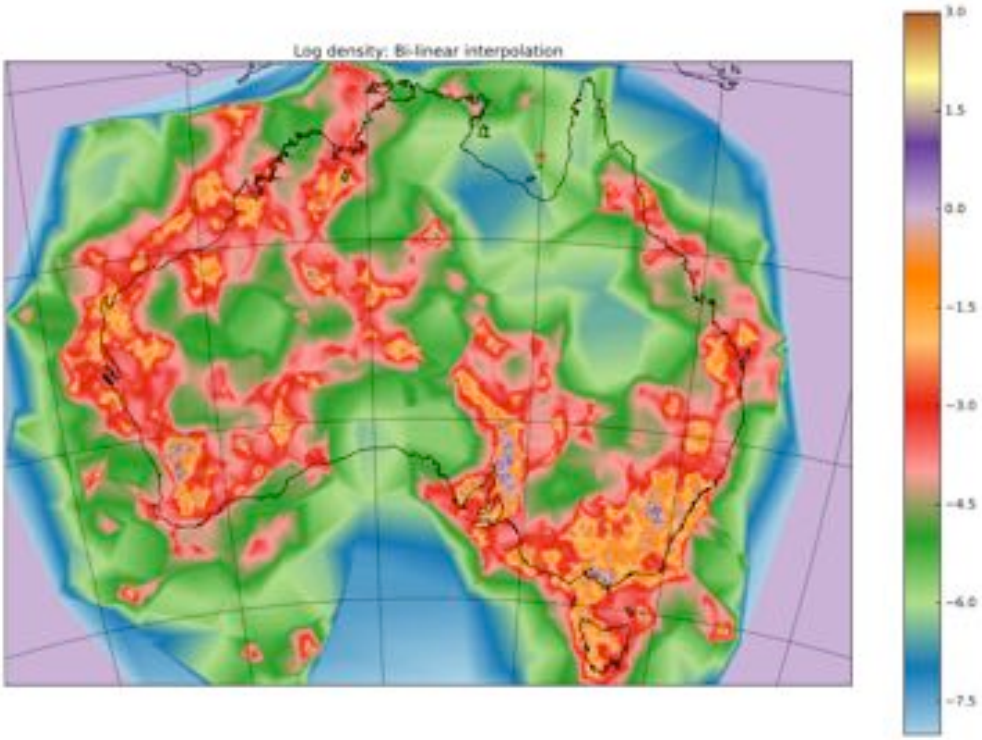

Figure 7 An interpolation of log-density proxy using a spatially bi-linear interpolation inside each Delaunay triangle. Here we see the first signs of smoothness in the interpolations, i.e. non zero second derivatives of the recovered log-density function.

The third interpolation is spatially bi-linear inside a triangulation of the earthquake epicentres, which provides the first degree of smoothness observable in the images[1]. This is seen in Figure 7.

2.4 Cubic interpolation using Hsieh-Clough-Tocher (HCT) elements

The fourth interpolation is spatially smooth and uses Hsieh-Clough-Tocher (HCT) elements. Figure 8 shows the image. This interpolation forces C1 smoothness on the interpolated image but remains faithful to the log-density proxy values at each earthquake location. The interpolation uses a Clough-Tocher subdivision scheme where each triangle is divided into three child-triangles, allowing the interpolated function to be a cubic polynomial of the two coordinates. This technique comes from the Finite Element literature (Bernadou and Hassan, 1988).

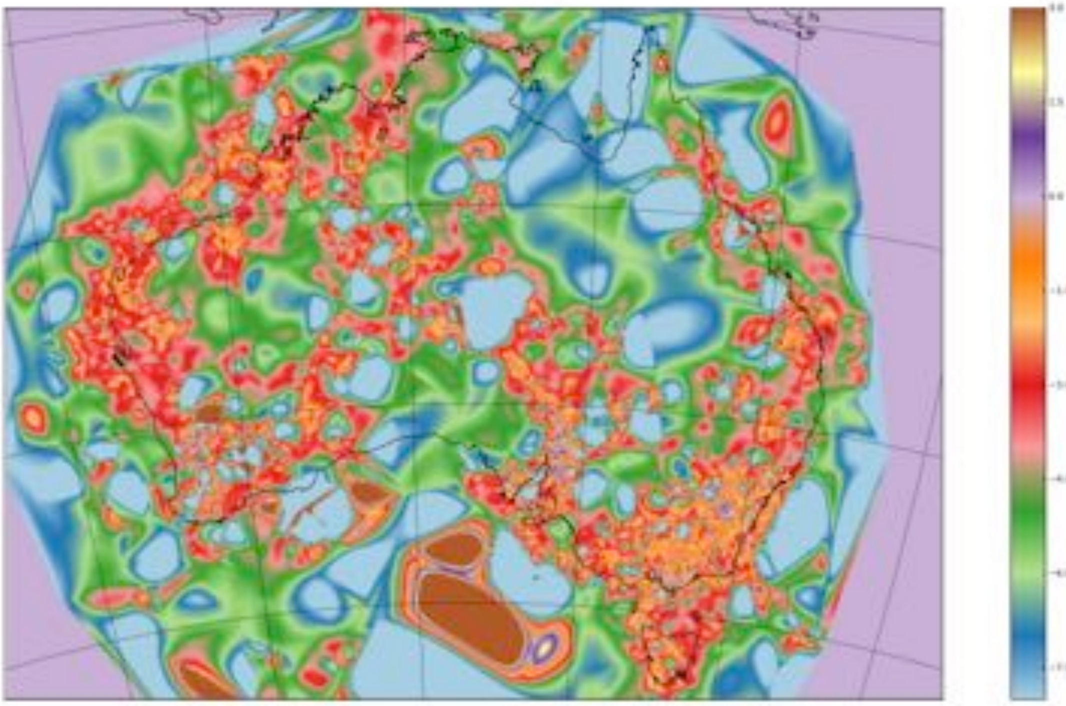

Figure 8 An interpolation of log-density proxy using Hsieh-Clough-Tocher (HCT) elements. This produces a C1 continuous function (i.e. the derivative exists and is differentiable).

In this image a smooth log-density field is produced. The highly variable multi-scale nature of the density variations results in high frequency variations that reflect local changes in seismicity. It is not clear how much of this variation is real. Its true multi-scale structure is also not clearly visible in simple plots such as Figure 8, and is better viewed with a dynamically re-scalable viewer where one can zoom into any scale. This is possible, for example, using windows created by the python programming language. Over and under shoots are visible in this image where the recovered function has exceeded the limits of the plotting range which are set at the extrema of the original log-density values from the Voronoi cells. These appear as high densities in the Australian Bight and low density `holes' in many other places. Such artefacts are common with interpolants that force the recovered density to vary smoothly such as HCT and may occur in regions where data density is relatively low. Nevertheless this produces a smooth continuous log-density image with continuous derivatives.

[1] This interpolation procedure is obtained from the python programming library scipy.interpolated.griddata using the `linear' method option.

2.5 Natural neighbour smoothing of Voronoi densities

The high frequency character and over-shooting of the image in Figure 8 suggests that it may be worth introducing some smoothing. Any regular spatial smoothing, e.g. spatial averaging of the density over a specified spatial distance scale, would destroy the multi-scale character of the information. With the Voronoi representation its possible to smooth this image in a manner consistent with its multi-scale nature using the Voronoi cells themselves as a smoothing operator. To do this we simply replace the log-density of each Voronoi cell with the mean of the log-densities of itself and neighbouring Voronoi cells. In Figure 2 this would mean replacing the log-density at node 1 with the average over itself and its six neigbouring cells labelled 5, 20, 13, 7, 14 and 3. This process is then repeated for each node/epicenter in the dataset. Since Voronoi cells have vastly varying sizes then the effect of this smoothing differs across the image. It results in smoothing over short spatial scales where the density is high and larger spatial scales where the density is low. This multi-scale smoothing filter can be applied any number of times, at each pass producing a slightly smoother image. Figure 9 shows HCT interpolation of density field produced after 9 passes of our multi-scale natural neighbour smoothing operator.

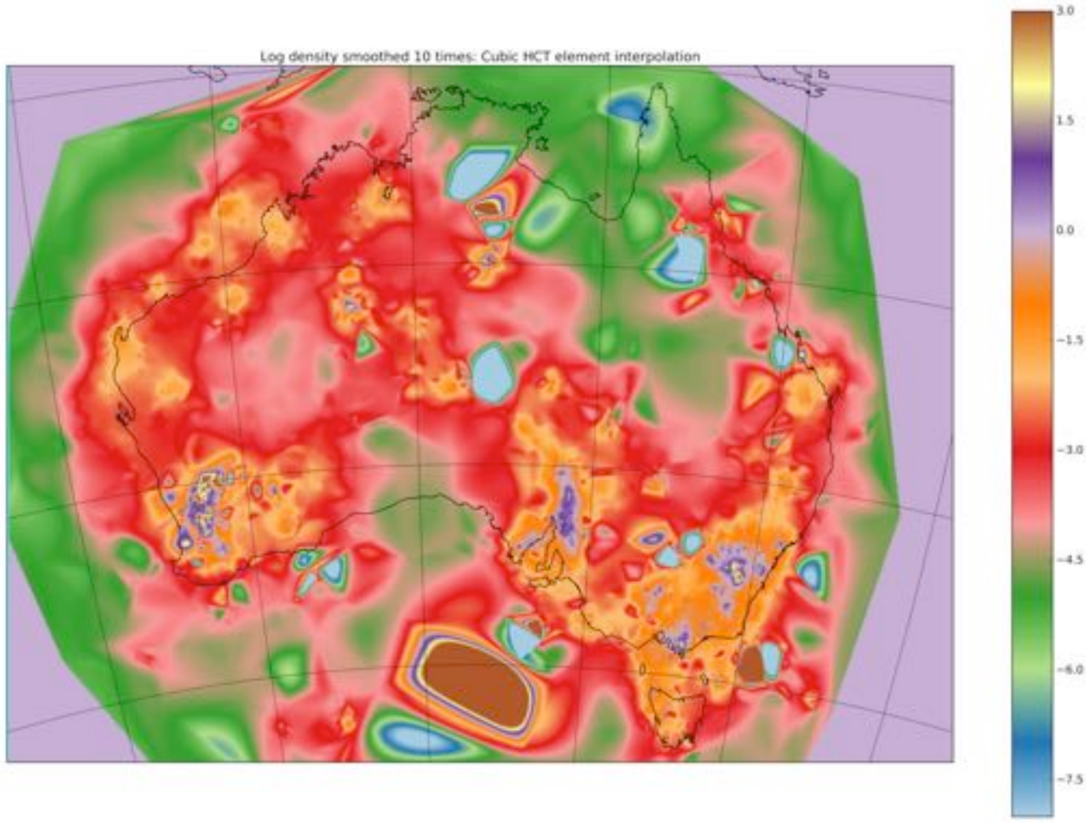

Figure 9 An interpolation of log-density proxy using Hsieh-Clough-Tocher (HCT) elements applied to natural neighbor smoothed densities. Nine passes of the natural neighbour smoothing have been applied. This produces a C1 continuous function.

As with Figure 8 some over and under-shooting as still present and clearly a few artefacts of the interpolation remain. See the unreasonably high densities in the Australian Bight and to the East of Tasmania, and a number of localized extreme low densities throughout the image. As an alternate we apply the linear interpolation method of Figure 7 to the 9 times log-density smoothed field. The result is shown in Figure 10.

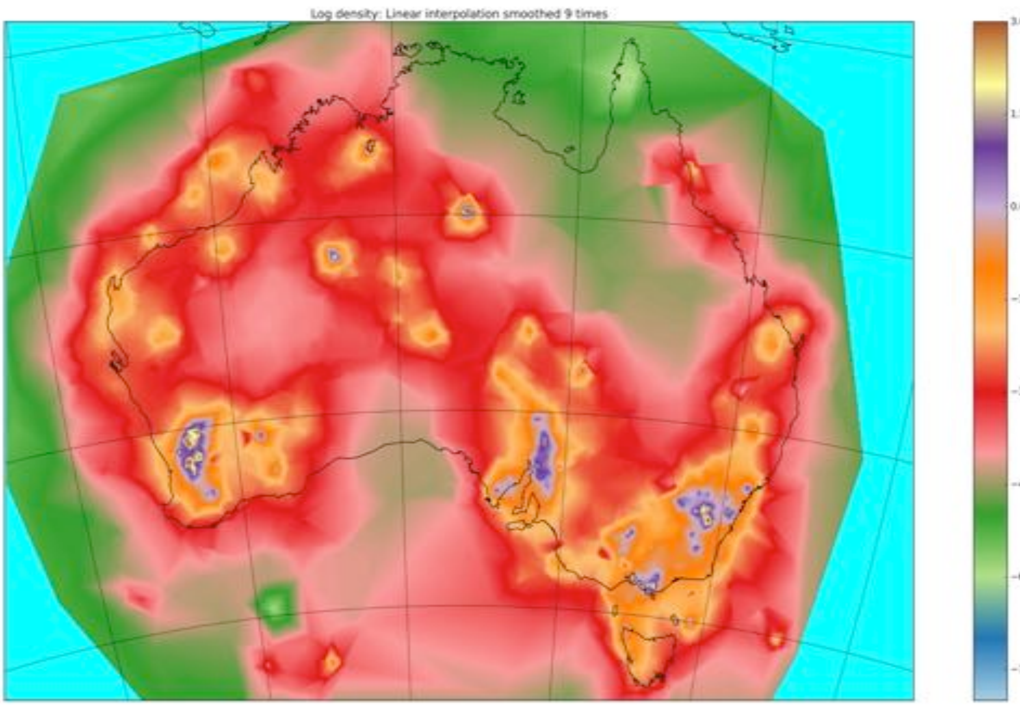

Figure 10 An interpolation of log-density proxy using linear interpolation applied to natural neighbor smoothed densities. Nine passes of the natural neighbour smoothing have been applied.

The choice of how many times the smoothing operator is applied is a subjective decision, varying from 1 when no smoothing is visible to 100 when all detail has been lost.

After investigating each of these interpolants, we favour the smoothed linear interpolant (Figure 10) as a source zone proxy because it gives a user defined smooth image of the log-density of epicentres that observes the multi-scale character of the data.

3. Discussion and Summary

We have proposed the geometric construct known as the Voronoi diagram, as an objective basis for calculation of spatially variable earthquake density estimates which may subsequently be used for zoning and probabilistic hazard analysis.

As the reader will note, our approach does not apply any weighting of each event in the construction of the Voronoi diagram and subsequent density estimate, taken as the inverse of Voronoi cell size, as in Figure 5. In particular no account is taken of earthquake magnitude and hence Figure 5 does not reflect seismic moment release. Earthquake magnitude is taken into account for zoning in the next phase of the hazard assessment process, when the recurrence relations and maximum magnitudes are derived (see Sinadinovski and McCue, this conference). Note that both fore- and aftershocks are included in the zoning process rather than being identified and removed. This is intentional. The number of foreshocks is minimal and plays little role in our examples, however by including aftershocks we ensure that larger earthquakes are effectively represented as an areal source rather than a single point source. The aftershocks are removed before the 'a' and 'b' values are computed in the recurrence relations.

Without an ad hoc choice of bin size or uniform smoothing within bins, our maps have been created using novel smoothing of log-density within neighbouring Voronoi cells. One of these maps, the linear interpolation (Figure 10) of log-density smoothed 9 times by averaging over natural neighbours could, for example, be used as an input for a PSHA model of continental Australia.

Our approach is not wholly judgment free, the one subjective choice is the number of iterations of the smoothing operator which is always a balance between fine detail (Figure 8) and total loss of detail. This should be viewed as a choice placed on top of the basic Voronoi diagram, rather than integral to it. Smoothing choices are open to improvement, but we argue that underlying Voronoi diagram is a novel and useful mechanism upon which to base such decisions.

4. Acknowledgments
The manuscript was improved by constructive feedback from two anonymous reviewers for which we are grateful.

5. References

Bernadou M. and K. Hassan, K., 1980. Basic functions for general Hsieh-Clough-Tocher triangles, complete or reduced. RR-0005, INRIA. https://hal.inria.fr/inria-00076556, 1980.

Brown, A., and Gibson G., 2004. A multi-tiered earthquake hazard model for Australia. Tectonophysics 390 (2004) 25– 43.

Cuthbertson, R., Jaumé, S., and Mora, P. 1997. The risk of earthquakes in Queensland and its urban centres: current estimates and predictions. UQ QUAKES Report #2.

Gaull, B.A., Michael-Leiba, M.O. and Rynn, J., 1990. Probabilistic earthquake risk maps of Australia. Australian Journal of Earth Sciences, **37**, 169-187.

Greenhalgh, S. A. and McDougall, R. M. 1990. Earthquake risk in South Australia . Civil Engineering Transactions 32(3):106-115.

Leonard, M., Clark, D., Collins, C. and McPherson, A., 2011. The 2012 Australian Seismic Hazard Map – Source Zones and Parameterisation. Proceedings of the 2011 Australian Earthquake Engineering Society Conference, Barossa Valley, SA.

Love, D., 1996. Seismic hazard and microzonation of the Adelaide metropolitan area. Report book 96/27 (unpublished) Department of Mines and Energy, South Australia.

McCue, K.F., 1973. On the seismicity of Western Australia, parts 1 and 2. Report of the Commonwealth Department of Works, Australia.

McCue, K.F., 1975. Seismicity and seismic risk in South Australia. University of Adelaide, Report ADP 137.

McCue, K., (compiler), Gibson, G., Michael-Leiba, M., Love, D., Cuthbertson, R., and Horoschun, G., 1993. Earthquake Hazard Map of Australia - 1991.

McCue, K. F. (1993). The revised Australian hazard map, 1991. Proceedings of the 1993 Australian Earthquake Engineering Society Conference, Sydney, NSW.

Okabe, A., Boots, B. and Sugihara, K., 1992. Spatial Tessellations Concepts and Applications of Voronoi Diagrams. John Wiley & Sons, Chichester, England, 1992.

Sambridge, M. S. Braun, J. and McQueen H. 1995. Geophysical parametrization and interpolation of irregular data using natural neighbours. Geophys. J. Int. 122:837–857, 1995.

Schäfer, A., and Daniell, J., 2014. A stochastic hazard assessment for Australia based on an external perspective. Australian Earthquake Engineering Society 2014 Conference, Nov 21-23, Lorne, Vic.

Schäfer, A.M. Daniell J.E. & Wenzel F. 2015. The seismic hazard of Australia - a venture into an uncertain future. Australian Earthquake Engineering Society. 2015 Conference, Nov 06-08, Sydney, NSW.

Scott, D. 1992. Multivariate Density Estimation: Theory, Practice, and Visualization. John Wiley & Sons, New York, Chicester, 1992.

Sinadinovski C., and McCue, K., 2016. A Proposed PSHA Source Zone for Australia. AEES Earthquake Engineering Society Conference, Nov 25-27, Melbourne, Victoria.

Voronoi M. G., 1908. Nouvelles applications des paramètres continus à la théorie des formes quadratiques. J. Reine Angew. Math., 134:198–287, 1908.